Original Research Article

Computational Investigation of Aerodynamic Forces on an Airfoil with Variations of the Reynolds Number and its Components

John Doan

Evergreen Valley High School, 3300 Quimby Rd, San Jose, CA 95148, United States

ABSTRACT

The lift force, drag force, and lift-to-drag ratio are essential performance metrics for any airfoil. Several studies have investigated these aerodynamic forces over a range of Reynolds numbers, but critically, detailed investigation of how the aerodynamic forces vary with response to independent changes in velocity, density and viscosity are scarce. Additionally, how the lift-to-drag ratio varies with the Reynolds number, *Re*, and individual variables within the Reynolds number is also unclear. In this study, computational fluid dynamics is used to assess the aerodynamic forces acting on an arbitrary airfoil over $3.3 \times 10^2 < Re < 6.8 \times 10^6$ by independently varying fluid velocity, density and viscosity. The lift-to-drag ratio was found to be approximately constant for $9.8 \times 10^5 < Re < 6.8 \times 10^6$. At $Re = 3.3 \times 10^4$, the lift-to-drag ratio was found to depend on the specific variables used to alter Re, likely due to shear force becoming more significant at low *Re*. Results from this work provide compelling evidence that the lift, drag, and lift-to-drag ratio vary not only as a result of variation of *Re* but also due to independent variation of components of *Re*. Future studies analyzing different metrics with respect to *Re* should specify what variables are varied to avoid ambiguity.

Keywords: Computational Fluid Dynamics; Aerodynamics; Reynolds number; Lift; Drag; Lift-to-drag; Airfoil

INTRODUCTION

When fluid flows past an object, the fluid exerts a force on it that can be split into two other distinct forces: the force caused by pressure differences in the surrounding fluid and the shear force caused by the fluid's viscosity. The former acts normal to the surface of the object and the latter acts tangential to the surface of the object. The sum of the components of these forces in the direction perpendicular and parallel to the relative motion of the object with respect to the fluid gives the lift and drag forces, respectively. The ratio of the lift force to the drag force acting on an object is the lift-to-drag ratio.

Airfoils are bodies – usually teardrop-shaped – that are optimized to produce more lift than drag in the air and thus produce high lift-to-drag ratios for flight. Almost all airborne vehicles utilize some sort of airfoil and as a result require the airfoil to be reliable and efficient. The Reynolds number, *Re*, effectively characterizes single-phase incompressible flow and is often used when studying flow around airfoils.

The Reynolds number is a dimensionless value that quantifies the ratio of inertial to viscous forces and predicts how fluid flows. It is given by $\rho UL/\mu$, where ρ is the fluid density (which is assumed to be uniform since

Corresponding author: John Doan, E-mail: johndoan428@gmail.com.

Accepted November 19, 2025
https://doi.org/10.70251/HYJR2348.36663669

only incompressible fluids are considered in this paper), U is the free stream velocity, L is the characteristic length, and μ is the dynamic viscosity of the fluid. In airfoils, the characteristic length is the length of the chord line, or the straight-line distance from the leading edge to the trailing edge of the airfoil. While the well-known equation for drag (external) forces on a body have a known dependency on fluid density and velocity, the drag equation contains an empirical parameter, the drag coefficient, which may change significantly across *Re.* Conventionally, this empirical parameter must be determined through experiments or simulation. Thus, the exact dependency on lift, drag, and lift-to-drag ratio on individual variables is not known *a priori.* Additionally, it is uncertain whether the sensitivity of the lift-to-drag ratio to individual variables (density, velocity, viscosity) will change with *Re*. This study investigates how individual variables within the Reynolds number affect the lift, drag, and lift-to-drag ratio on a standard airfoil using CFD.

Aerodynamic efficiency, typically expressed as the lift-to-drag ratio (L/D), remains a central metric in airfoil performance analysis. Foundational theories have shaped our understanding of this ratio, beginning with Prandtl's lifting-line theory (1), which models the spanwise lift distribution and explains the origin of induced drag in finite wings. His later work on minimizing induced drag (2) established the elliptical lift distribution as an ideal for drag reduction under constrained conditions. Complementing this, von Kármán's boundary layer theory (3) provides the theoretical basis for analyzing viscous drag, particularly in the transition from laminar to turbulent flow. These classical frameworks remain directly relevant to modern CFD studies, offering essential context for interpreting simulated aerodynamic behavior.

In a study conducted by Schewe (4), the effect of *Re* on the lift and drag coefficients of an airfoil at high angle of attack was analyzed. For constant fluid density and velocity, the aerodynamic coefficients are directly proportional to their corresponding aerodynamic forces (5). The study observed a sharp decrease and increase in the drag and lift coefficient respectively in the region of *Re* of the airfoil in which laminar flow transitions to turbulent flow. The scope of the data in this paper is expected to fall in this transcritical range of *Re*.

Variations in aerodynamic coefficients with respect to has also been done on airfoils involving Gurney flaps. According to Jain *et al*. (6), lift coefficients for the NACA 0012 with Gurney flaps are higher than those without flaps for all tested Reynolds numbers (5.0×10^4 to 3.0×10^5) and angles of attack (0° to 16°). The study suggests that the lift coefficient decreases as *Re* decreases up until aerodynamic stall, for airfoils with and without Gurney flaps. For airfoils without Gurney flaps, the lift coefficient varies more at high angles of attack than at low ones, where airfoils experienced "negligible changes" in the lift coefficient. The study also found that the drag coefficient increases as *Re* decreases for both airfoil types and that its variation is independent of the angle of attack. Airfoils with Gurney flaps experience less of an increase in the drag coefficient than standard airfoils. Something to point out about this study is that it is unclear what variable within *Re* was changed to adjust the value during testing. Perhaps if a variable other than the one altered in the study was changed, then a different outcome would have been observed.

Leishman (7) found that the lift coefficient of the NACA 4412 airfoil varied almost linearly with angle of attack for $1 \times 10^5 < Re < 3 \times 10^6$ and that it varied nonlinearly below $Re = 1 \times 10^5$. The nonlinearity at lower *Re* is due to the thicker boundary layers and long laminar separation bubbles above the airfoil, both of which contribute to increased drag and reduced lift. Leishman also found that decreasing *Re* at lower lift coefficients resulted in a sharp increase in drag at a certain point, which agrees with existing literature and findings. Further, Leishman (7) found that at a fixed angle of attack, lift coefficient increases with *Re* over the range $20000 < Re < 75000$, before plateauing at approximately $Re = 70000$. In a similar CFD study, Mazumder *et al.* found that the lift-to-drag ratio remains approximately constant across moderate Reynolds numbers for certain NACA airfoils (8).

In this study, the lift, drag, and lift-to-drag ratio of a model airfoil is investigated using computational fluid dynamics over a wide range of Reynolds numbers. To vary the Reynolds number, density, viscosity, and velocity of the fluid were all varied. The results give insight into (i) the dependence of lift, drag, and lift-to-drag ratio on *Re*, and (ii) how those metrics can be influenced by different combinations of the same *Re*, expanding on the significance of *Re* on aerodynamic performance and testing.

METHODS AND MATERIALS

To conduct computational fluid dynamics simulations, Flowsquare was used (9). Flowsquare is a two-dimensional computational fluid dynamics software that

can simulate unsteady flows, and was used as it is a free and readily accessible CFD tool which can be applied to study single phase flow for simple geometries. In this study, it was used to simulate incompressible fluid flow of varying fluid viscosity, free stream velocity, and density around an airfoil. The software simulates the flow field around any arbitrary body by first splitting the field into a grid of $n_x \times n_y$ mesh points. For each mesh point the Flowsquare solves the Navier-Stokes equations for incompressible flow, given by:

$$\nabla \cdot u = 0$$

$$\rho \frac{du}{dt} = -\nabla p + \mu \nabla^2 u + F$$

where ∇ is the divergence, u is the fluid velocity field, ρ is the fluid density, p is the fluid pressure, and F is all of the external forces on the observed fluid particle. A detailed explanation of the calculations can be found in the "User's Guide" in Flowsquare by Minamoto (9). Note that Flowsquare does not handle any sub-grid turbulence model, and therefore the effect of any sub-grid turbulence is not captured.

After this process is completed for all mesh points, the simulation is advanced by a time (which is typically on the order of microseconds) and the Navier-Stokes equations are solved again in these new conditions. In the end, Flowsquare creates a fluid simulation around an arbitrary body that changes with respect to time.

To calculate the lift and drag force on the airfoil after a simulation, a separate numerical code (written in C) from Flowsquare was used that takes pressure and velocity data from the simulation and computes the net force acting on the body by integrating both the shear and normal contributions across the total exposed area (10). The program uses the trapezoidal rule for integration, and returns the sums of the lift and drag components acting on the airfoil. This code was used to post-process all simulation results to obtain the lift and drag force. In all cases, the results (pressure and velocity fields) from the final time-step in the simulation were used.

The airfoil analyzed in this paper is available on Flowsquare and shown in Figure 1. Although the type of airfoil is not specified, it approximately resembles a NACA 2412: a well-known airfoil used in several operating aircraft such as the Cessna 172 and the Ikarus C42 (11).

The dimensions used in the simulation are 9.0 m × 4.5 m. To calculate accurate Reynolds numbers for each simulation, the characteristic length L (chord length) was needed. By manually measuring the horizontal and vertical dimensions of the airfoil and using the Pythagorean theorem, the chord length was calculated to be 3.26 m.

The computational domain of 9.0 m × 4.5 m was discretized into 512 × 256 grid points. The time step of the simulation was controlled by setting the delta t factor in Flowsquare to 8, and 20000 time steps were conducted to ensure proper convergence of the simulation (which was verified visually in all cases). The initial conditions of the simulation corresponded to setting the pressure throughout the flow domain to atmospheric pressure and the velocity to the inlet velocity, and the density to the density of the fluid in the appropriate case. At the inlet, a boundary condition was set with certain initial parameters specified for each simulation. On the surface of the airfoil, a no-slip boundary condition was used to represent the wall. Flowsquare solved the incompressible Navier-Stokes equations by discretizing the equations using 4th order finite difference method in conjunction with the Lax-Wendroff method (12).

Each variable of *Re* (with the exception of the characteristic length) was varied one at a time and increased at regular intervals, starting from the base case provided by Flowsquare. Each variation produced a value of *Re* that corresponded to two other runs with the same *Re* but varied another variable. These values of the parameters used for all case studies conducted are reported in Table 1. After a number of variations, the setup was adjusted to analyze the aerodynamic forces at a low (3.3×10^5) but identical *Re*. The final two simulations aimed to analyze the aerodynamics at the lowest possible *Re* the software could handle without convergence issues.

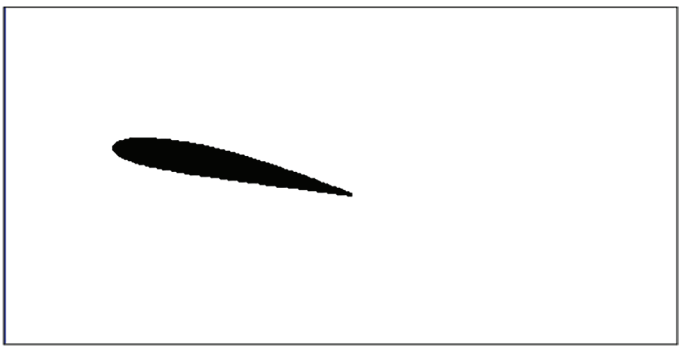

Figure 1. The airfoil, approximately a NACA 2412, which was used for all simulations conducted in this study.

RESULTS

Table 1 details the parameters used for each simulation and the corresponding aerodynamic forces and lift-to-drag ratio. Lift force and drag force were computed as outlined in the Methods section. All lift, drag, and lift-to-drag ratio values in Table 1 are reported to two significant figures. Key trends in the data reported in Table 1 are presented and discussed later in Figures 4 through 6.

Figures 2 and 3 show the final pressure and velocity fields from case study #1 (the base case) respectively. Simulations were saved every 40 time steps, according to the specific parameters given in the table.

Figures 4 and 5 show graphs of lift and drag force as

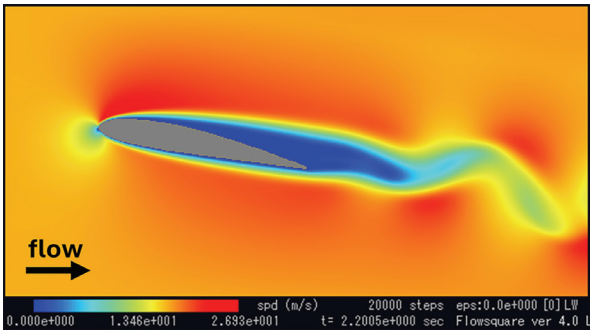

Figure 2. The final velocity field for the first case study, measured after 20,000 time steps for flow around Flowsquare's default airfoil at $Re = 3.9 \times 10^6$. The fluid's density and viscosity are 1.20 kg/m^3 and 0.000020 $Pa \cdot s$ respectively, initially moving at 20.00 m/s.

Table 1. Configurations used in simulations and resulting lift, drag, and lift-to-drag ratio.

case study #	ρ [kg/m^3]	μ [Pa · s]	u [m/s]	L [m]	Re [-]	F_L [N]	F_D [N]	F_L/F_D [-]
1	1.20	0.000020	20.00	3.26	3.9E+06	2.0E+02	9.1E+01	2.2
2	0.30	0.000020	20.00	3.26	9.8E+05	5.0E+01	2.3E+01	2.2
3	0.60	0.000020	20.00	3.26	2.0E+06	1.0E+02	4.5E+01	2.2
4	0.90	0.000020	20.00	3.26	2.9E+06	1.5E+02	6.8E+01	2.2
5	1.50	0.000020	20.00	3.26	4.9E+06	2.5E+02	1.1E+02	2.2
6	1.80	0.000020	20.00	3.26	5.9E+06	3.0E+02	1.4E+02	2.2
7	2.10	0.000020	20.00	3.26	6.8E+06	3.5E+02	1.6E+02	2.2
8	1.20	0.000020	5.00	3.26	9.8E+05	1.3E+01	5.7E+00	2.2
9	1.20	0.000020	10.00	3.26	2.0E+06	5.0E+01	2.3E+01	2.2
10	1.20	0.000020	15.00	3.26	2.9E+06	1.1E+02	5.1E+01	2.2
11	1.20	0.000020	25.00	3.26	4.9E+06	3.2E+02	1.4E+02	2.2
12	1.20	0.000020	30.00	3.26	5.9E+06	4.5E+02	2.0E+02	2.2
13	1.20	0.000020	35.00	3.26	6.8E+06	6.2E+02	2.8E+02	2.2
14	1.20	0.000080	20.00	3.26	9.8E+05	2.0E+02	9.1E+01	2.2
15	1.20	0.000040	20.00	3.26	2.0E+06	2.0E+02	9.1E+01	2.2
16	1.20	0.000027	20.00	3.26	2.9E+06	2.0E+02	9.1E+01	2.2
17	1.20	0.000016	20.00	3.26	4.9E+06	2.0E+02	9.1E+01	2.2
18	1.20	0.000013	20.00	3.26	5.9E+06	2.0E+02	9.1E+01	2.2
19	1.20	0.000011	20.00	3.26	6.8E+06	2.0E+02	9.1E+01	2.2
20	0.01	0.000020	20.00	3.26	3.3E+04	2.0E+00	7.4E-01	2.7
21	1.20	0.002400	20.00	3.26	3.3E+04	2.1E+02	9.2E+01	2.2
22	1.20	0.000020	0.17	3.26	3.3E+04	3.0E-02	1.1E-02	2.7
27	1.20	0.024000	20.00	3.26	3.3E+03	2.0E+02	8.9E+01	2.2
28	1.20	0.240000	20.00	3.26	3.3E+02	2.1E+02	1.1E+02	1.9

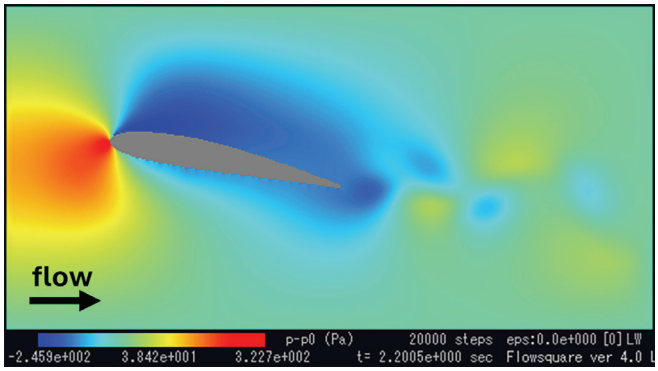

Figure 3. The final pressure field for the first case study, measured after 20,000 time steps for flow around Flowsquare's default airfoil at $Re = 3.9 \times 10^6$. The fluid's density and viscosity are 1.20 kg/m^3 and 0.000020 $Pa \cdot s$ respectively, initially moving at 20.00 m/s.

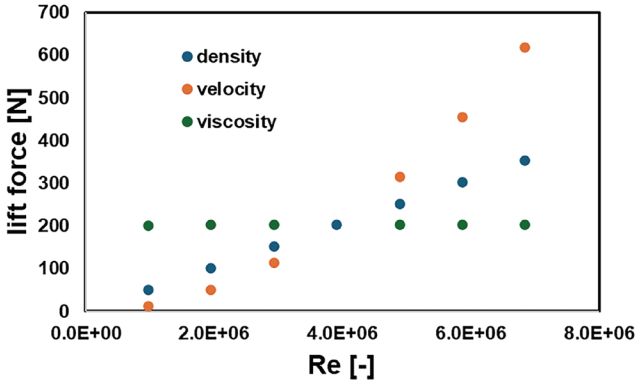

Figure 4. Lift force as a function of *Re* for flow over (approximate) NACA 2412 airfoil. Density, velocity, and viscosity were varied independently to achieve variation in *Re*, and are shown as different series. Lift force was computed from the velocity and pressure field results of CFD simulations.

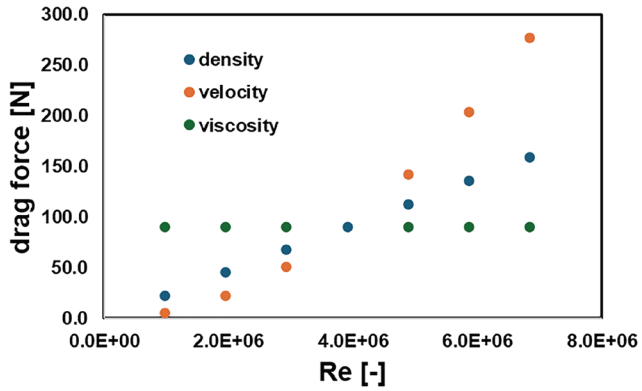

Figure 5. Drag force as a function of *Re* for flow over (approximate) NACA 2412 airfoil. Density, velocity, and viscosity were varied independently to achieve variation in *Re*, and are shown as different series. Drag force was computed from the velocity and pressure field results of CFD simulations.

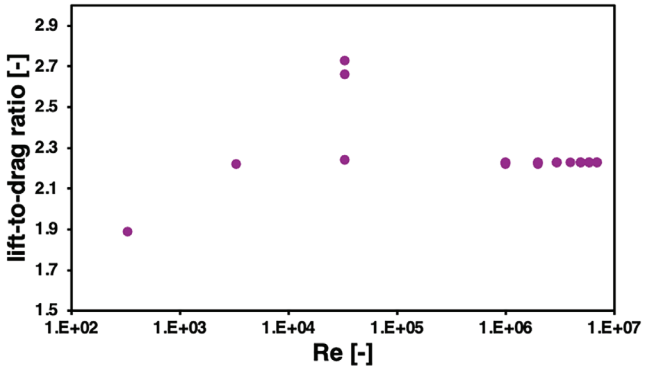

Figure 6. Lift-to-drag ratio as a function of *Re* for flow over (approximate) NACA 2412 airfoil. Lift and drag forces were computed from the velocity and pressure field results of CFD simulations.

a function of *Re* for the first 19 simulations (Table 1). The aerodynamic forces appear to vary quadratically with fluid velocity, linearly with fluid density, and remain constant with viscosity. Such variation is approximately consistent with constant lift and drag coefficients, which also depend on velocity, density, and viscosity in the same way.

Figure 6 shows the effect of *Re* on the lift-to-drag ratio for all simulations on a logarithmic scale. At $9.8 \times 10^5 < Re < 6.8 \times 10^6$, the lift-to-drag ratio is roughly constant at 2.23. At $Re = 3.3 \times 10^5$, adjusting different variables in *Re* to reach the designated value resulted in a different lift-to-drag ratio. At the lowest tested value of *Re*, achieved by increasing the fluid viscosity, the lift-to-drag ratio dropped to 1.89, over 15% less than the relatively stable value of the ratio at higher magnitudes of *Re*. Inspection of the results for this case study in Table 1 shows that the change in lift-to-drag ratio for the lowest *Re* case tested was caused by a strong increase in the drag force (due to the high viscosity).

DISCUSSION

The manner in which the lift and drag force vary with changes in density and velocity reflect the corresponding force equations, namely:

$$F = \frac{1}{2}\rho u^2 CA$$

where F is the lift or drag force, C is the lift or drag coefficient, and A is the reference area (5). The insensitivity of the lift and drag forces and the lift-to-drag ratio to changes in viscosity at high Re reflect its relatively insignificant effect on the shear forces and thus its absence in the lift and drag force equation.

However, at the lowest Re studied in this paper (3.3×10^2), fluid viscosity is increased by approximately 4 orders of magnitude, drastically increasing the significance of the shear forces on the airfoil. This consequently increases drag more than lift and decreases the lift-to-drag ratio by a considerable amount, suggesting that viscosity plays a larger role in airfoil performance at lower Re as viscous forces become more significant relative to inertial forces. For micro-air-vehicle and UAV designs, the effects of fluid viscosity on performance must be considered if the medium is relatively viscous, since smaller objects have a lower resistance to acceleration from external forces and the viscosity of the medium could significantly change the trajectory of smaller aerial vehicles. However, for common mediums such as air and water, viscosity is generally not relatively high and its effects can thus be considered to be negligible.

The constancy of the lift-to-drag ratio for $9.8 \times 10^5 < Re < 6.8 \times 10^6$ implies that at this range of Re the variables affect both forces on an arbitrary airfoil equally. At $Re = 3.3 \times 10^5$, fluid velocity, density, and viscosity increased the lift-to-drag ratio from the most to least respectively. This suggests a positive correlation between the sensitivity of the lift-to-drag ratio and the significance of specific variables in the lift and drag force equation at lower Re – that is, $F = \frac{1}{2}\rho u^2 CA$.

CONCLUSION

Based on simulation results from Flowsquare, this paper concludes that different variables of Re affect the aerodynamic forces and lift-to-drag ratio on an airfoil differently – namely, variables will affect the aerodynamic forces according to their significance in the lift and drag force equation. The lift-to-drag ratio also stays roughly constant at a value of 2.2 for $9.8 \times 10^5 < Re < 6.8 \times 10^6$, but breaks down at extremely low Re (3.3×10^2), at which the ratio drops to 1.9. This implies the significance of viscous forces in the calculation of aerodynamic forces, contrary to the absence of viscosity in the corresponding equation. Additionally, the increase in the lift-to-drag ratio at lower Re appears to depend on the specific variable altered. Limitations in this study include, but are not limited to, the use of relatively dated CFD software, the assumption of fluid incompressibility that comes with calculating aerodynamic forces with the incompressible Navier-Stokes equations, and the lack of detailed sub-grid turbulence modelling used in this work. This work provides clear evidence that lift, drag, and the lift-to-drag ratio depend not only on the Reynolds number but also on its underlying variables – density, viscosity, and velocity – which has implications for the design and analysis of future aerodynamics studies. Future work should extend this analysis to compressible flow regimes and alternative airfoil geometries.

CONFLICT OF INTEREST

The author declares that there are no conflicts of interest related to this work.

REFERENCES

1. Prandtl L. Tragflügeltheorie. I. Mitteilung. Nachr Ges Wiss Göttingen, Math-Phys Kl. 1918; 1918: 451-477.
2. Prandtl L. Über Tragflügel kleinsten induzierten Widerstandes. Z. Flugtech. Motorluftsch. 1933; 24: 1–8.
3. von Kármán T. Über laminare und turbulente Reibung. *Z. Angew. Math. Mech.* 1921; 1 (4): 233–252. https://doi.org/10.1002/zamm.19210010401
4. Schewe G. Reynolds-number effects in flow around more-or-less bluff bodies. *J. Wind Eng. Ind. Aerodyn*. 2001; 89 (14–15): 1267–89. doi:10.1016/s0167-6105(01)00158-1
5. Benson T. Density effects on aerodynamic forces. (online). NASA. Available from: http://www.grc.nasa.gov/WWW/k-12/VirtualAero/BottleRocket/airplane/density.html (accessed on 2025-8-30)
6. Jain S, Sitaram N, Krishnaswamy S. Effect of Reynolds number on aerodynamics of airfoil with gurney flap. *Int. J. Rotat. Mach*. 2015; 2015: 1–10. doi: 10.1155/2015/628632
7. Leishman JG. Aerodynamics of airfoil sections. (online). Embry-Riddle Aeronautical University: Daytona Beach FL; 2023. Available from: https://eagle-pubs.erau.edu/introductiontoaerospaceflightvehicles/chapter/airfoil-characteristics/ (accessed on 2025-9-21)
8. Mazumder MH, Rahman MM, Hossain MA. CFD analysis of NACA airfoils for wind turbine and aero-

space applications at low Reynolds numbers. *Int. J. Adv. Sci. Eng. Technol.* 2024; 9 (1): 1–6. https://doi.org/10.21203/rs.3.rs-4965405/v1

9. Minamoto Y. Flowsquare 4.0: theory and computation. (online). Flowsquare; 2013. Available from: http://flowsquare.com/Download4/Users_Guide.pdf (accessed on 2025-7-30)
10. Anderson JD Jr. Aircraft performance and design. Boston MA: McGraw-Hill Higher Education; 2012.
11. Lednicer D. The incomplete guide to airfoil usage. (online). University of Illinois Urbana-Champaign: Urbana-Champaign IL; 1998. Available from: https://m-selig.ae.illinois.edu/ads/aircraft.html (accessed on 2025-9-9)
12. Lax P, Wendroff B. Systems of conservation laws. Commun. *Pure Appl. Math.* 1960; 13 (2): 217–37. doi: 10.1002/cpa.3160130205